PCCP

PAPER

Cite this: *Phys. Chem. Chem. Phys.*, 2015, **17**, 30648

Radiation-induced transformations of matrix-isolated formic acid: evidence for the HCOOH → HOCO + H channel

Sergey V. Ryazantsev and Vladimir I. Feldman*

Received 11th September 2015,
Accepted 22nd October 2015

DOI: 10.1039/c5cp05446j

www.rsc.org/pccp

The effect of X-ray irradiation on the isolated formic acid molecules (HCOOH) in solid noble gas matrices (Xe, Kr, Ar, and Ne) at very low temperatures (6 K) was first studied by FTIR spectroscopy. Carbon oxides (CO and CO_2) and hydrocarboxyl radicals (HOCO) have been detected as the principal degradation products. The formation of HOCO radicals represents a primary dissociation channel for formic acid, which was not reported previously under UV photolysis in solids. This reaction can be explained by the involvement of the recombination-induced excited states, which are not populated in photolysis. The effects of the matrix and the absorbed dose on the product formation were studied in detail and possible mechanisms are discussed with particular attention to the difference between radiolysis and UV-photolysis of the matrix-isolated formic acid. The results obtained provide a new insight into the effects of high-energy impact on the simplest carboxylic acid with possible implications to the astrochemical problems, in particular, the prebiotic evolution in the interstellar medium.

Introduction

Formic acid, one of the simplest organic molecules, is among the most popular species for model spectroscopic and photochemical studies focusing on different aspects (elucidation of the effects of intermolecular interactions and complexation, dynamics of rotational isomerization, basic mechanisms of photolysis of small molecules, *etc.*). The evolution of formic acid under the action of UV light and ionizing radiation is of particular interest for atmospheric and interstellar chemistry. The photoinduced transformations of formic acid were extensively investigated for several decades, both in the gas phase and in solid media.[1–14] Regarding photodissociation channels, there is a remarkable difference between the processes observed in the gas phase and in low-temperature matrices. In the former case, UV photolysis (193–225 nm) leads to predominant dissociation of OH and HCO radicals:[3–6]

$$\mathrm{HCOOH} \rightarrow \mathrm{HCO} + \mathrm{OH} \quad (1)$$

On the other hand, UV irradiation of the matrix-isolated formic acid results in dissociation *via* two channels:[10,11,13]

$$\mathrm{HCOOH} \rightarrow \mathrm{H_2O} + \mathrm{CO} \quad (2)$$

$$\mathrm{HCOOH} \rightarrow \mathrm{H_2} + \mathrm{CO_2} \quad (3)$$

It is worth noting that the ratio between reactions (2) and (3) is strongly matrix-dependent.[10,11] Furthermore, it was found that these channels were remarkably selective for *trans*- and *cis*-conformers of the formic acid, which is a prominent example of fine control of photochemical reactions in the solid phase.[12] In addition to experimental studies, the photodissociation dynamics of formic acid was a topic of extensive theoretical studies.[6,11,15–21]

The effect of high-energy (ionizing) radiation on formic acid is much less studied. Meanwhile, the radiation-driven chemistry of HCOOH in the condensed phase may be directly relevant to the most intriguing problems of astrochemistry and prebiotic evolution of matter since formic acid is an important component of interstellar and cometary ices.[22,23] Several astrochemically targeted studies on the transformations of formic acid under the action of soft X-rays, electrons, and energetic ions were published during the past decade.[24–28] The decomposition products were characterized mainly by mass spectrometry and related techniques. More recently, Andrade *et al.* reported a FTIR study on the effect of energetic heavy ions on the formic acid ice at 13 K,[29] which is an important step in modelling chemical evolution of this molecule in an interstellar environment. Nevertheless, it is worth noting that IR spectroscopic characterization of all the products and intermediate species in irradiated molecular ices is hardly possible, because their features may be masked by extremely strong absorptions of the parent substance. Furthermore, it is often difficult to judge about the detailed reaction mechanism only from the spectroscopic data obtained in icy molecular solids due to complexity of the systems (especially, in mixed ices) and high irradiation doses typically used in such studies.

Department of Chemistry, Lomonosov Moscow State University, Moscow 119991, Russia. E-mail: feldman@rad.chem.msu.ru

The matrix isolation studies may be very helpful in these aspects since they provide rich and precise spectroscopic information. Moreover, in certain cases, it is possible to follow the fate of the primary radiation-induced intermediates by monitoring the annealing behaviour. In fact, the matrix isolation approach was extensively applied for simulation of light-induced transformations of various astrochemically important species, including simple molecules, radicals and complexes. Particularly relevant to this study, one can refer to a very recent work on the simulation of the photochemical evolution of the HCOOH–CH_3CN system using a solid neon matrix.[30] However, the matrix isolation studies on the effect of ionizing radiation on organic molecules are still rather limited and, to the best of our knowledge, there are no reports on the radiolysis of formic acid in solid noble gas matrices.

An approach developed in our laboratory is based on a combination of FTIR and EPR spectroscopy as applied to characterization of the radiation-induced transformations of matrix isolated molecules occurring under the action of fast electrons or X-rays in solid deposited films.[31–33] Our early studies were mainly related to hydrocarbons and some other medium size organic molecules.[31–39] Important general findings of these studies were concerned with significant difference in the mechanisms of the radiation-induced and photochemical transformations of the studied molecules and very strong and specific effects of the matrix host on the degradation of guest molecules. Recently, we used a similar technique to study the radiation-induced chemical evolution of small molecules and complexes directly relevant to atmospheric and interstellar chemistry.[40] In the latter case, FTIR spectroscopy was the method of choice since it is particularly sensitive to intermolecular interactions and makes it possible to follow simultaneously the degradation of the parent molecules and the formation of the radiolysis products (both paramagnetic and diamagnetic). Here we report the first systematic investigation on the radiation chemistry of isolated formic acid in different solid noble gas matrices (from neon to xenon). This work aims at two main targets: (i) to compare the relative yields of degradation products and matrix effects for the radiolysis and photolysis of matrix isolated formic acid and (ii) to explore the occurrence of additional decomposition channels (unknown from photochemical studies) in view of their possible implications to hot problems of astrochemistry. In particular, this study was partially motivated by a search for the formation of the HOCO radical, either directly or as a result of secondary reactions found in our recent investigations on the irradiated CO_2/H_2O/M systems (M = Ar, Kr, or Xe).[40] This fundamentally important four-atomic species (a carbon-centered radical, also referred as a COOH, hydroxycarbonyl, or hydrocarboxyl radical) is directly relevant to the formic acid. An indication of the C–H bond rupture leading to HOCO was found under photodissociation of HCOOH in the gas phase.[7,8] However, to our knowledge, it was not reported previously in any study on the HCOOH photochemistry in solid matrices.

Experimental

Our experimental approach of radiation-chemical experiments in solid noble gas (Ng) matrices doped with guest molecules has been generally described elsewhere.[34,40–44] Formic acid vapours were mixed with an excess amount of an appropriate noble gas in a glass vacuum line following a standard manometric technique. Xe (99.9996%), Kr (99.99%), Ar (99.998%) and Ne (99.996%) were used as received for the preparation of the mixtures with the typical HCOOH to Ng ratio of 1 : 1000 (the ratio of 1 : 2500 was used in the case of a HCOOH/Ne sample). Additional experiment examining the effect of an electron scavenger ($CFCl_3$, 99.9%) on the formic acid decomposition was performed with a HCOOH/$CFCl_3$/Kr 1 : 1 : 1000 sample. Special care was taken of the effect of absorption–desorption of the formic acid in the glass elements of our experimental set-up during mixture preparation and matrix deposition since HCOOH is known to be easily adsorbed on the glass walls.[45] The procedure included saturation of glass walls of the system with HCOOH vapour through several filling–keeping–evacuating cycles one day prior to its use for the mixture preparation/deposition. Ignoring such arrangements led to the virtual absence of observable formic acid in deposited matrix samples, whereas the experiments carried out immediately after saturation (without a one-day delay) yielded poor-quality matrices containing large clusters of formic acid instead of the formic acid monomer. On the other hand, following this procedure we were able to obtain reproducible, highly monomeric matrices.

Matrix-isolation experiments were performed using an original closed-cycle helium cryostat based on an SHI RDK-101E cryocooler (the principle scheme and description could be found in ref. 44). The sample temperature was controlled using a *t*-STAT 310xcm device (RTI Cryomagnetic Systems, Russia) connected to the calibrated Cu : Cu(Fe) thermocouple, or a LakeShore 325 temperature controller connected to the calibrated Cernox™-type sensor. The prepared gas mixtures were deposited slowly onto a cold KBr substrate by passing through the deposition vacuum line and the flux was adjusted using a needle valve. Whereas the deposition of the neon matrix was carried out at the lowest available temperature of the substrate (*ca.* 6 K), the deposition temperature was 14, 20 and 24 K for Ar, Kr and Xe matrices, respectively, to compromise between optical quality of the sample and the aggregation of isolated molecules. Typical layer thickness (as monitored by the interference pattern) was *ca.* 60–100 μm for Xe, Kr and Ar matrices after a one-hour deposition. Since neon is a rather poor absorber of X-ray radiation (see below), in this case, we prepared a thicker sample (*ca.* 150 μm) of a more diluted mixture (1 : 2500 as was mentioned above) in order to increase the total absorbed dose in the sample with similar absorption intensities. After deposition, the samples were irradiated with X-rays using a 5-BKhV-6(W) tube with a tungsten anode (typical voltage 32 kV; anode current, 70 mA; effective energy *ca.* 20 keV). The irradiation time varied between 3 and 150 minutes, depending on the matrix material. Matrices were irradiated through a 50 μm Al-foil window at the lowest attainable temperature (*ca.* 6 K).

The FTIR spectra were recorded at 6 K using a PerkinElmer 1720X FTIR-spectrometer (MCT detector, 4000–400 cm^{-1} range, resolution of 1 cm^{-1}, averaging by 200 scans). At the end of experiments, the samples were warmed up to 44 K (for the

xenon matrix) or 34 K (for krypton and argon matrices), annealed during 5 minutes and then cooled down again to measure the resulting spectra.

Results

IR spectroscopy of formic acid in noble gas matrices is well described in the literature.[10,11,46–56] In complete agreement with the previously reported data, we observed all the fundamental absorptions of *trans*-HCOOH in the IR-spectra of deposited samples. The corresponding data are given in Table 1. A metastable *cis*-confomer of formic acid was not detected in the deposited samples. We also observed a number of weak absorptions, which should be attributed to *t*-HCOOH dimers and *t*-HCOOH···H_2O intermolecular complexes (isolated water was also observed in our spectra since it is a common impurity in matrix samples). The assignment in different matrices was made on the basis of previously reported spectroscopic data on such complexes of *t*-HCOOH isolated in solid argon, taking into account reasonable matrix shifts.[50,52,53] The spectroscopic data for these species are also collected in Table 1. We refer to different structures of formic acid dimers as *tt*-1, *tt*-2 and *tt*-3 following the nomenclature suggested previously.[53]

X-ray irradiation of the deposited matrix samples resulted in significant decay of formic acid molecules and simultaneous appearance of several new absorptions from the radiolysis products, as illustrated in Fig. 1 (with the example of krypton (a) and argon (b) matrices). The new bands arising in the spectra of irradiated samples correspond to the formation of CO_2 (peaks at 2334.5, 2336.8, 2345.6, 659.6 and 3587.5 cm^{-1} in Xe; 2340.4, 660.4 and 3595.7 cm^{-1} in Kr; 2344.8, 2342.9, 2340.0, 662.3 and 3602.5 cm^{-1} in Ar; and 2347.3 and 668.1 cm^{-1} in Ne), $^{13}CO_2$ (2269.2 and 2271.6 cm^{-1} in Xe, 2275.0 cm^{-1} in Kr; 2279.4 and 2277.2 cm^{-1} in Ar; and 2281.8 cm^{-1} in Ne), CO (2133.0 cm^{-1} with shoulder 2137.0 cm^{-1} in Xe; 2135.5 cm^{-1} in Kr; 2138.3 cm^{-1} in Ar; and 2141.0 cm^{-1} in Ne), its complexes with H_2O (2127.4 and 2141.3 cm^{-1} in Xe; 2130.1, 2145.0 and 2140.6 cm^{-1} in Kr; 2149.0 and 2151.8 cm^{-1} in Ar; and progression of bands in the range of 2161–2143 cm^{-1} in Ne) and *t*-HOCO radicals (1834.2, 1210.0, 1202.5 and 1063.2 cm^{-1} in Xe; 3581.7, 1839.7 with shoulder at 1836.1, 1210.8, 1206.0 and 1065.0 cm^{-1} in Kr; 1843.7 with shoulder at 1840.1, 1211.2, 1208.9 and 1064.7 cm^{-1} in Ar; 1847.7 and 1210.7 cm^{-1} in Ne).[10,11,40,57] These species occurred in all the studied matrices, however, their relative yields showed strong variations depending on the matrix nature, as will be discussed below. It is worth noting that both CO and CO_2 (although in significantly different proportions) were observed in previous matrix isolation photochemical studies, whereas the HOCO radical was not found as a product of formic acid photolysis in any matrix.[10,11] We can also notice that radiolysis led to the predominant formation of isolated CO molecules (especially, after relatively long exposure), whereas H_2O···CO complexes were mainly found after photolysis.[10,11] In addition to the species mentioned above, irradiation of formic acid in argon, krypton and xenon also resulted in the appearance of the progressions of low-frequency bands corresponding to positive ions ArH^+Ar (903.3 and 1139.6 cm^{-1}), KrH^+Kr (852.5, 1007.7, and 1160.4 cm^{-1}) and XeH^+Xe (730.6, 842.7, and 953.4 cm^{-1}) respectively.[58] All these features are well-known from the previous studies and they occur under photolysis or radiolysis of different hydrogenated molecules in noble gas matrices.

Table 1 Absorption maxima (in cm^{-1}) of *t*-HCOOH and its complexes in noble gas solids. For *t*-HCOOH···H_2O and $(HCOOH)_2$ values in parentheses are the data reported previously in ref. 52 and 53

Species	Mode	Ne	Ar	Kr	Xe
t-HCOOH	ν_1(O–H_{str})	3569.0	3550.2; 3548.2	3536.5; 3529.8	3521.2; 3513.0
	ν_2(C–H_{str})	2937.7	2952.7; 2955.5	2944.5	2931.2
	ν_3(C═O_{str})	1773.5	1767.2	1762.6	1757.1
	ν_4(C–H_{rock})	1379.6	1381.1	1378.4	1375.1
	ν_5(CO–COH_{def})	1217.4	1215.5	1211.6	1213.5; 1207.2
	ν_6(COH–CO_{def})	1102.6	1103.7; 1106.7	1101.2; 1104.9	1097.6; 1101.3
	ν_8(C–H_{wag})	1035.7	1038.3	1036.0	1032.6
	ν_9(COH_{tors})	637.9	635.5; 638.7	633.0; 637.5	631.0; 635.4
	ν_7(OCO_{sci})	626.2	629.3	628.1	625.5; 626.7
t-HCOOH···H_2O	ν_1(O–H_{str})	3221.5; 3206.7	3211.8 (3212)	—	—
	ν_2(C–H_{str})	2930.0	2944.1 (2944)	—	—
	ν_3(C═O_{str})	1743.3	1737.4 (1737)	1737.9	1732.0
	ν_6(COH–CO_{def})	1177.4	1172.5 (1172)	1174.6	1170.8
	ν_9(COH_{tors})	833.5	828.9 (829)	832.2	834.5
$(HCOOH)_2$ *tt*-1	ν_1(O–H_{str})	3077.1	3072.0 (3072)	3063.9	—
	ν_3(C═O_{str})	1737.2	1728.4 (1728)	1727.3	1722.8
	ν_6(COH–CO_{def})	1224.3	1227.0 (1225)	1220.4; 1217.4	—
$(HCOOH)_2$ *tt*-2	ν_3(C═O_{str})	1754.0	1747.9 (1748)	1745.1	1741.4
	ν_6(COH–CO_{def})	1130.2	1131.5 (1131)	1128.0	1123.0
	ν_9(COH_{tors})	661.1	657.9 (658)	656.5	653.1
$(HCOOH)_2$ *tt*-3	ν_3(C═O_{str})	1770.9	1764.9 (1765)	—	—
	ν_6(COH–CO_{def})	1117.3	1114.8 (1114.6)	1112.5	—

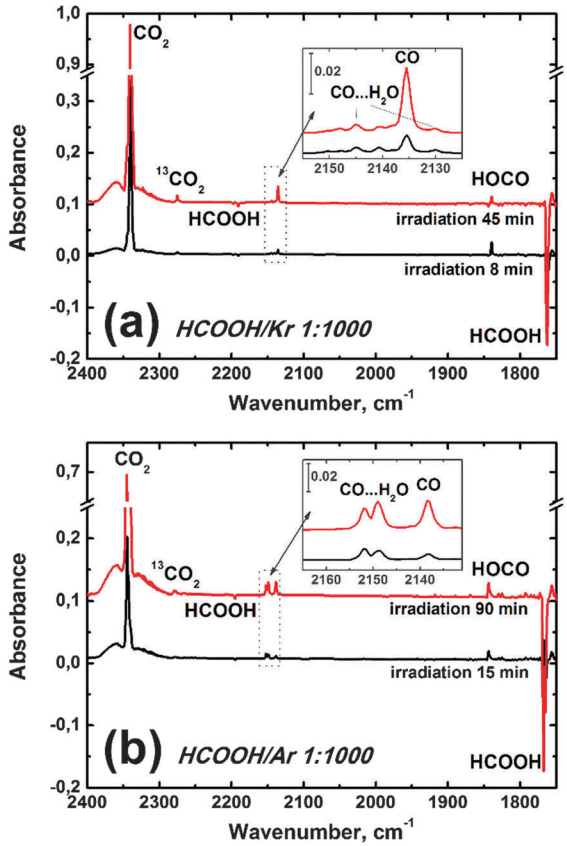

Fig. 1 Difference IR spectra illustrating the effect of X-ray irradiation of (a) HCOOH/Kr and (b) HCOOH/Ar samples.

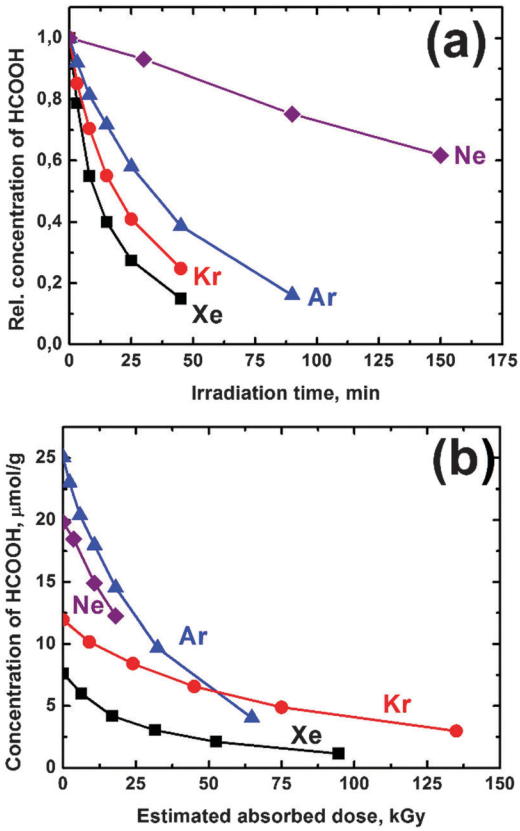

Fig. 2 The rate of radiation-induced decay of HCOOH as a function of irradiation time (a) and estimated absorbed dose (b). Relative concentration of formic acid in (a) was determined by integration of ν_2 absorption of HCOOH in the corresponding FTIR spectra. The molar mass concentration in (b) was calculated on the basis of initial mixture composition. Estimated absorbed dose values rely on dosimetry data for our experimental system (ref. 43).

The rate of the radiation-induced decomposition of formic acid is strongly matrix-dependent, as shown in Fig. 2a, so, in the cases of heavy matrices (krypton and xenon), even a relatively short X-ray exposition (*ca.* 30 min) was sufficient for the decomposition of more than 50% of parent molecules. At a qualitative level, this effect is expected taking into account that X-ray irradiation is mainly absorbed by a matrix, which results in a drastic difference in the absorbed dose rate in different matrices. Indeed, in the case of X-ray photons used in our study ($E_{\mathrm{eff}} \sim 20$ keV), the dominant absorption mechanism is the photoelectric effect and the absorption cross-section depends strongly on the atomic number of the matrix material (Z). However, the quantitative interpretation is not so straightforward. The mass absorption coefficients for the X-rays with $E = 20$ keV are 1.317, 8.074, 35.09, and 24.65 $\mathrm{cm^2\ g^{-1}}$ for neon, argon, krypton, and xenon, respectively.[59] If we take these values as a measure of the effective dose rate in the corresponding matrices, the decomposition of formic acid may be represented as a function of the absorbed dose as shown in Fig. 2b. Note that in this case the amount of formic acid is represented in molar mass concentration, because the dose is energy absorbed per a mass unit. From this picture, we can see that the actual trend in the decomposition efficiency normalized to the absorbed energy (relative radiation-chemical yields) is quite different from that shown in Fig. 2a. In fact, the decomposition yields estimated from the initial slopes of the curves given in Fig. 2b for argon and neon matrices are roughly twice higher than those found for krypton and xenon. One possible explanation of this difference may be concerned with rather large uncertainty in these values. Indeed, the attenuation half-length for 20 keV photons is *ca.* 3000, 450, 40 and 70 μm for Ne, Ar, Kr and Xe respectively (calculated using data from ref. 59). Considering typical thickness of the matrix deposited layer (*ca.* 60–100 μm, see the Experimental section), one may conclude that the dose rate is nearly uniformly distributed in "light" matrices (neon and argon), virtually transparent for the X-rays used. However, in the case of xenon and krypton, the dose distribution is strongly non-uniform since the layer thickness is comparable with the attenuation length. In addition, using single value of effective energy instead of a real wide X-ray spectrum is not a good approximation for heavy atoms with deep electronic levels. Both these reasons would lead to overestimation of the absorbed dose in krypton and xenon using a simplified approach based on the value of the mass absorption coefficient at specific photon energy. Taking into account this effect, we may figure out that the decomposition efficiency for formic acid is roughly comparable in different noble gas matrices.

In order to overcome this uncertainty for quantitative comparison of the efficiency of product formation, we have used invariant coordinates (relative absorption intensity *vs.* degree of

the HCOOH decomposition) in further consideration. This simply means that in each case we compare the proportion of decomposed molecules yielding a given product in different matrices. Evaluation of the relative yields of the observed products also requires the knowledge of integrated absorption coefficients. Following the approach used in ref. 11 and 12, we assumed a 10/1 ratio for the absorption coefficients of the absorptions corresponding to CO_2 (stretching) and CO. The total amount of CO was evaluated by integration of the absorptions of both CO monomers and CO···H_2O complexes (see above), taking into account that the absorption coefficient is not affected much by the formation of a complex.[12] Since we are unaware of any experimental data on the HOCO absorption coefficient, we used the best known computed value based on a high-level calculation of the IR absorption intensities in comparison with the known value for CO.[60,61] This yields roughly a 3/1 ratio for CO_2/HOCO integrated absorption intensities in the C═O stretching region.

Whereas the dose dependence of formic acid decomposition follows a simple exponential law, the kinetics of product formation demonstrates different behavior. The corresponding data are presented in Fig. 3(a–d) in convenient invariant coordinates. They reflect apparent involvement of the secondary processes at higher doses. Possible explanations will be discussed below.

An important characteristic for comparison with photolysis is the branch ratio of the CO_2/CO production channels. Fig. 4 presents the corresponding data as a function of conversion degree. One can see that the initial ratio increases strongly when going from neon to xenon. Furthermore in the case of xenon, this ratio shows pronounced dose dependence, decreasing at high does. The origin of these effects will be discussed in detail in the next section.

We have also examined the effect of an electron scavenger (Freon-11) on the radiolysis of formic acid in a krypton matrix (1/1/1000). In this case, the decomposition of HCOOH was five times slower in comparison with that in the sample containing the same concentration of formic acid without Freon. We observed similar products of formic acid degradation, but the relative yield of HOCO was several times lower, while the CO_2/CO ratio changed only slightly (within 20%). The effect of the electron scavenger as well as the matrix effect on a relative HOCO yield are presented in Fig. 5.

Annealing of the irradiated samples leads to the formation of a new species due to the reaction of mobilized hydrogen atoms produced under the radiation-induced decomposition of HCOOH, either directly or through the formation of H_2O followed by its decomposition at higher doses. H atoms react with isolated molecules (residual HCOOH or produced CO) yielding *trans*-H_2COOH (IR absorption bands at 957.9 and 959.5 cm^{-1} in Xe, 962.2 and 964.7 cm^{-1} in Kr, and 965.2 and

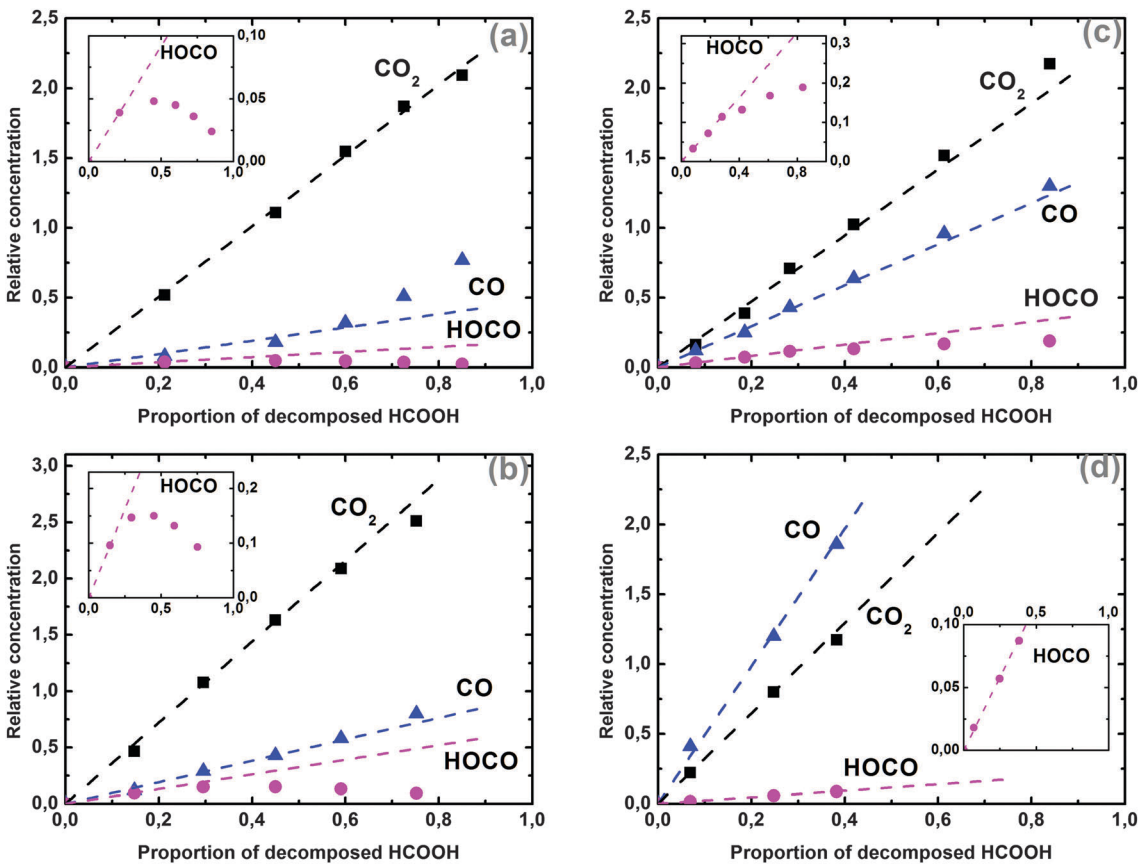

Fig. 3 Build-up profiles of CO_2, CO and HOCO generated from the radiolysis of formic acid in (a) Xe, (b) Kr, (c) Ar and (d) Ne matrices. Relative concentrations were determined from integrated IR absorptions in the C═O_{str} stretching region multiplied by a corresponding coefficient (1 for CO_2, 3 for HOCO and 10 for CO). Dashed lines reflect initial slopes of the observed profiles.

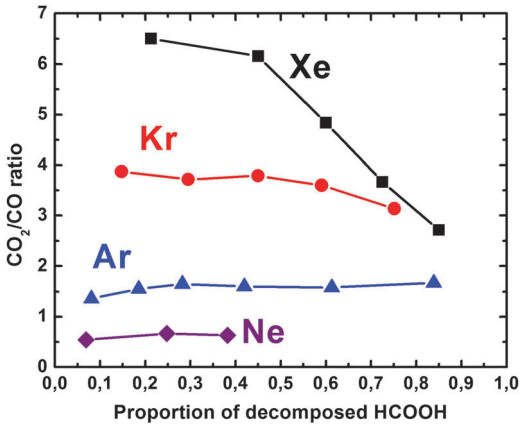

Fig. 4 Effects of the matrix material and the absorbed dose on the branching ratio of CO_2 and CO production channels during radiolysis of matrix-isolated formic acid.

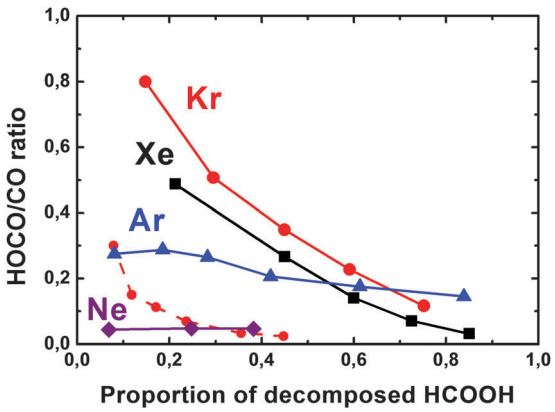

Fig. 5 Effects of the matrix material and the absorbed dose on the branching ratio of HOCO and CO production channels during radiolysis of matrix-isolated formic acid. Dashed line corresponds to the krypton matrix doped with Freon-11.

967.5 cm^{-1} in Ar), HCO (1856.3 cm^{-1} in Xe, 1860.1 cm^{-1} in Kr, and 1863.5 cm^{-1} in Ar) and its complex with water (1849.8 cm^{-1} in Xe, 1853.2 cm^{-1} in Kr, and 1853.8 cm^{-1} in Ar).[62,63] In the case of xenon matrices, the formation of HXeH molecules (doublet with maxima at 1166.5 and 1181.1 cm^{-1})[64,65] was also observed upon increasing the temperature of irradiated samples. Slight decay of HOCO absorption was observed upon annealing. However, we did not observe any annealing-induced absorptions, which could be assigned to the new noble gas compounds of the type HNgCOOH or HCOONgH.[66] Probable pathways leading to HOCO decay are H + HOCO → H_2O + CO and H + HOCO → H_2 + CO_2.[67] However, it is difficult to evaluate the contributions of these channels, because CO also reacts with H atoms and concentration of CO_2 is much greater than that of HOCO.

Discussion

Reaction mechanisms: radiolysis *vs.* photolysis

Comparing our results on the radiation-induced degradation of formic acid in matrices with the previously reported data on the UV-photolysis, we can emphasize two most important features. First, we have obtained evidence for the formation of HOCO, which was not detected in photochemical studies. Regarding possible origin of this species, generally, one should consider the possibility of its appearance in primary or secondary processes. Indeed, recently we found HOCO as a product of the radiation-induced evolution of $CO_2\cdots H_2O$ intermolecular complexes[40] and one cannot exclude similar transformation for $CO\cdots H_2O$ or $CO_2\cdots H_2$ complexes produced under decomposition of formic acid. However, the kinetics of HOCO formation observed in the present study (Fig. 3) reveals the absence of the induction period and therefore suggests that it results from a primary process. It means that we deal with a new, previously unreported degradation channel for HCOOH in solid matrices:

$$HCOOH \rightarrow HOCO + H \quad (4)$$

It is worth noting that the production of H atoms was observed in the gas-phase studies on UV-photodissociation of formic acid and it was attributed to the involvement of reaction (4) occurring at the T_1 potential surface of HCOOH.[7,8]

Although the yield of channel (4) in our studies is not large (as compared to the CO_2 formation), the HOCO radical is clearly seen in all the matrices. Furthermore, in the cases of argon and krypton, the intensity of the major HOCO absorption at low doses is comparable with that of CO, or even higher. From the initial slopes of the dose dependencies (Fig. 3), we can roughly extract the relative contribution of reaction (4) in the radiation-induced degradation of formic acid in different matrices: ~3% in Ne, ~10% in Ar, ~12% in Kr, and ~6% in Xe.

The second feature is strong difference in the relative yields of two major reaction channels (the formation of CO and CO_2) between photolysis and radiolysis. Indeed, in the case of 193 nm photolysis of *t*-HCOOH, the CO/CO_2 ratio was found to be ~5 : 1 (Ar), ~4 : 1 (Kr), and ~0.7 : 1 (Xe),[11] whereas in our experiments we have obtained the following values of initial relative yields (Fig. 3): ~1.5 : 1 (Ne), ~0.6 : 1 (Ar), ~0.3 : 1 (Kr), and ~0.2 : 1 (Xe). In other words, in the case of radiolysis, the formation of CO_2 predominates in all the matrices, except for neon.

In order to understand the observed difference between photolysis and radiolysis, one should consider the mechanisms of both processes in detail. UV photolysis results in direct excitation of the isolated formic acid molecules. In the case of 193 nm photolysis, it implies the primary population of the lowest singlet excited state (S_1) and it is this state that is responsible for the predominating formation of CO in light matrices.[11] The formation of triplet states under optical excitation is a spin-forbidden process, so its probability is very low. However, such states can be populated through the intersystem crossing, which becomes effective in the matrices with a high atomic number *Z* (in particular, in xenon) due to much stronger spin–orbit coupling. Taking into account this external heavy atom effect, high yield of CO_2 in xenon was explained by its formation from a triplet excited states (presumably, T_2).[11] Thus, the reaction channels (2) and (3) under photolysis were attributed to different precursor spin states. It is worth nothing that none of these states yield the HOCO radical.

As mentioned above, the degradation mechanism of the matrix isolated molecules under radiolysis is significantly different. Detailed consideration of the radiation-induced processes occurring under such conditions is given elsewhere.[31–34] The basic physical feature is that the ionizing radiation energy is primarily absorbed by the matrix and the isolated molecules are activated mainly due to charge and excitation transfer. The difference between the radiation-driven chemistry and photochemistry in matrices results from possible involvement of the ionic reaction channels and population of the optically unattainable states in the former case. A general formal scheme of possible radiation-induced processes for formic acid in the noble gas matrices may be written as follows:

$$M \rightsquigarrow M^+, M^*, e^- \quad (5)$$

$$M^+ + HCOOH \rightarrow HCOOH^+ + M \quad (6)$$

$$M^* + HCOOH \rightarrow HCOOH^* + M \quad (7)$$

$$HCOOH^+ + e^- \rightarrow HCOOH^{**} \quad (8)$$

$$HCOOH + e^- \rightarrow [HCOOH^-]\,(?) \rightarrow \text{products} \quad (9)$$

$$HCOOH^+ \rightarrow \text{products} \quad (10)$$

$$HCOOH^* \rightarrow \text{products} \quad (11)$$

$$HCOOH^{**} \rightarrow \text{products} \quad (12)$$

Here M denotes a noble gas atom (Ne, Ar, Kr, or Xe) and X* or X** means an electronically excited state (X** is used particularly for the recombination-induced excited states, independent of their spin multiplicity). It is worth noting that the primary process (5) implies not only direct absorption of an X-ray photon, but mainly interaction with secondary electrons (in the case of 20 keV X-rays, each primary photon produces *ca.* 10^3 secondary electrons). Reactions (6) and (7) describe positive hole transfer and exciton transfer, respectively. These processes are basically responsible for activation of the matrix isolated molecules under radiolysis. The positive hole transfer is determined by the difference in the ionization potentials (ΔIP) between the matrix atom and the isolated guest molecule (the latter species acts as a hole trap). According to the previous studies,[31–34] the distant positive hole transfer in solid noble gas matrices is quite efficient, provided that the ΔIP value is, at least, 1.5–2 eV. Since IP(HCOOH) = 11.33 eV,[68] this is definitely the case for Ne, Ar, and Kr matrices (IP = 21.56, 15.76, and 14.0 eV for Ne, Ar, and Kr, respectively).[68] Meanwhile, in the case of Xe (IP = 12.13 eV,[68] ΔIP = 0.8 eV), the situation is uncertain. We will refer to this feature in further discussion of matrix effects.

Reaction (9) formally describes an interaction of HCOOH molecules with low-energy excess electrons. Possible role of this channel is, in fact, questionable. While the HCOOH molecule has no intrinsic electron affinity,[69] most probably, it cannot scavenge thermalized excess electrons in non-polar, low polarizable matrices, as it was shown for some other carbonyl compounds.[70] Indeed, there is no evidence for stabilization of the $HCOOH^-$ radical anion in any noble gas matrix studied in this work. On the other hand, in general, one cannot exclude dissociative electron attachment (DEA) due to the reaction of formic acid molecules with low-energy non-thermal secondary electrons. The processes of such kind were shown to occur in ultrathin organic films subjected to the impact of low-energy electron beams (E = 1–10 eV).[71] However, to the best of our knowledge, their role in the solid state radiation chemistry in matrices is not confirmed yet. Anyway, in the present study we did not obtain clear evidence for the formation of significant amounts of anionic fragments, which might result from reaction (9).

The fate of the primary radical cation $HCOOH^+$ should depend on its excess energy.[31–34] This excess energy basically results from high exothermicity of the positive hole transfer (6), which may be characterized by the above-mentioned ΔIP value. It was shown previously[31–33,36] that some organic radical cations produced by radiolysis in a solid argon matrix at ΔIP > 5 eV underwent rapid fragmentation, which competed favorably with the ion–electron recombination. This "hot" fragmentation at low temperatures was less effective in krypton and virtually negligible in xenon, which was explained by simultaneous decrease of the ΔIP value and increase in the matrix polarizability facilitating excess energy relaxation, while turning from argon to xenon.[33,36] More detailed studies revealed that the "hot" fragmentation of radical cations in argon is sensitive to the peculiarities of their molecular structure and, in certain cases, it does not occur even at high ΔIP, probably due to effective internal redistribution of excess energy followed by its dissipation to the matrix lattice.[36,38] In any case, one might expect fragmentation of $HCOOH^+$ preferentially in neon (ΔIP ∼ 10 eV) and, less probable, in argon (ΔIP ∼ 4.4 eV). Actually, regarding the cationic species, we have found only very weak features, which may be attributed to $HCOOH^+$ and $HOCO^+$ in solid neon, and no definite signs of primary or fragment cations in other matrices.

From the above-given consideration we may suggest that the observed products of radiolysis result mainly from the exciton-induced and recombination-induced neutral excited states (HCOOH* and HCOOH**, respectively). With this preliminary conclusion, we can focus on possible explanations of the two above-mentioned features of the radiolysis mechanism.

The actual spectrum of excited states produced under radiolysis is not known, so further discussion is somewhat speculative. Nevertheless, it is clear that both kinds of these excitations may involve the states, which are not populated under direct optical transitions. In particular, the spin multiplicity of the recombination states having ionic precursors is determined by the spin correlation between the hole and electron species. If an ion–electron pair results from a single molecule, this should be a spin-correlated state leading to a singlet excited state upon recombination. Alternatively, if the recombination involves random pairs originating from different precursors (no spin correlation), it yields both triplet and singlet excited states with the limiting population ratio T/S = 3/1 determined by the spin statistics. As stated above, in the case of matrix isolation under high dilution, the primary matrix hole should typically migrate over a long distance (more than ten lattice periods) to find a guest molecule, and the electron also travels a long distance before thermalization. Thus, quite likely, the recombination process (8) involves

non-correlated ion–electron pairs, which should lead to significant or predominating formation of triplet excited states. Furthermore, there should be a significant contribution of high-energy triplet states with $E \sim$ IP, which cannot be produced by intersystem crossing from the S_1 state populated in photolysis. Our previous studies on the radiolysis of hydrocarbons and ethers in noble gas matrices suggest that the recombination excited states formed in these systems mainly dissociate *via* the C–H bond cleavage: $RH^{**} \rightarrow R + H$.[31,33,39] This conclusion was particularly illustrative in the case of benzene, which produced high yield of phenyl (C_6H_5) radicals and trapped H atoms under radiolysis in solid xenon,[39] in sharp contrast with benzene photolysis in any matrix. The result was tentatively explained by involvement of high triplet excited states unattainable in photolysis. We believe that similar explanation can be applied to the formation of HOCO radicals from formic acid observed in this work. This process may include internal conversion of higher triplets to a vibrationally hot T_1 state. According to recent theoretical studies, the reaction channel yielding HOCO from the T_1 state is characterized by a barrier of *ca.* 0.4 eV,[15,21] whereas there are no reliable calculations for high triplet excited states.

Another important peculiarity of radiolysis is the high relative yield of CO_2 in all the matrices (in comparison with photolysis). It can be reasonably explained by larger probability of population of the T_2 triplet excited states (similar to that produced by intersystem crossing under HCOOH photolysis in xenon). In the case of radiolysis, such states may result from both triplet exciton transfer (7) and ion–electron recombination (8). On the other hand, we cannot exclude the additional formation of CO_2 from higher singlet states, which are not populated under a 193 nm photolysis, or vibrationally hot species.

The proposed mechanism is partially supported by the experiment with an electron scavenger (Freon-11). This experiment was carried out in a krypton matrix producing the highest relative yield of the HOCO radical, which is in focus of our study. According to our previous studies,[31–33] addition of an electron scavenger typically leads to strong suppression of the products resulting from the recombination excited states due to electron capture precluding the ion–electron recombination. Simultaneously, high yields of guest radical cations or products of their reaction are often observed in the presence of electrons scavengers.[32–36] The interpretation of the results for a HCOOH/$CFCl_3$/Kr system is not that straightforward. First, substantial decrease in the degradation rate of formic acid in the presence of Freon-11 may be explained by the competition between HCOOH and $CFCl_3$ for the holes and electrons produced in the matrix. Indeed, we observed the formation of the radicals and ions produced from Freon molecules (detailed analysis is out of the scope of this paper). Second, a noticeable suppression of the relative yield of HOCO in the presence of the scavenger supports our preliminary conclusion about the formation of this species through the triplet states resulting from charge recombination. Meanwhile, at first glance, two facts remain unexplained, namely, the absence of trapped radical cations $HCOOH^+$ in the presence of Freon and the small effect of the electron scavenger on the CO/CO_2 production ratio. The latter result may seem surprising, as we suppose that CO_2 results, at least partially, from the triplet excited states produced by the ion–electron recombination. To understand both these findings, we may suggest that the $HCOOH^+$ radical cation escaping recombination in the presence of an electron scavenger undergoes deprotonation to krypton:

$$HCOOH^+ + 2Kr \rightarrow HCOO + KrH^+Kr \quad (13)$$

Indeed, the deprotonation reaction of this kind was demonstrated for some oxygen-centered radical cations in solid xenon and krypton matrices. In such cases, only deprotonation products (radicals) were found instead of the primary radical cation in the presence of electron scavengers.[33,37] It is worth noting that deprotonation (13) is supposed to be a relatively slow reaction in comparison with the ion–electron recombination (8) since the products of this reaction are clearly observed only in the presence of electron scavengers.[33] Furthermore, it was assumed that extremely acidic radical cations, like CH_4^+, H_2O^+, or CH_3OH^+, could undergo deprotonation to the matrix even in argon and that is the reason, why these species were observed only in the neon matrix,[72] which has the lowest polarizability. To the best of our knowledge, the $HCOOH^+$ radical cation was also observed previously only in a neon matrix.[57] Thus, it may belong to the same row, so its deprotonation to krypton looks quite probable. If it is the case, the resulting HCOO (formyloxyl) radical is not stabilized in the matrix because of rapid decarboxylation to yield CO_2 and H atoms.[45]

$$HCOO \rightarrow H + CO_2 \quad (14)$$

This reaction may explain why the yield of CO_2 is actually not suppressed in the presence of Freon.

Effects of matrix and secondary reactions

As shown in the Results section, the relative yield of the observed products (CO, CO_2, and HOCO) demonstrates strong dependence on the matrix used. Taking into account the above-described mechanisms, we may try to interpret the effect of the noble gas matrix on the radiolysis of formic acid. At first glance, the formation of HOCO radicals follows a rather unexpected trend: Ne < Ar ~ Kr > Xe. Obviously, there is no correlation with the matrix Z number. This finding provides additional evidence that the precursor states are not populated through intersystem crossing, but result from some other mechanism (in line with the proposed scheme). We believe that the values obtained in Ar and Kr correspond to ''normal'' contribution of high triplet excited states produced by recombination, whereas the yields in Ne and Xe are low for different reasons. In the case of neon, the primary $HCOOH^+$ radical cations possess high excess energy ($E_{ex} \sim \Delta IP \sim 10$ eV, see above), so a considerable fraction of these species may not survive to recombination because of ''hot'' fragmentation. A relatively weak point of this explanation is that we did not observe noticeable yields of the products of ionic fragmentation. However, we should take into account that the total yield of the formic acid degradation in neon is rather low (even for the longest irradiation time) and an expected contribution of the ionic fragmentation in the total

degradation is 10% or less. Thus, the absorptions of the products of this channel may be too weak to be reliably detected.

On the other hand, in the case of xenon, the formation of $HCOOH^+$ may be inefficient because of small ΔIP (see subsection "Reaction mechanisms: radiolysis *vs.* photolysis"). A similar situation occurs, for example, for acetylene in xenon.[73] In such systems the matrix holes mainly undergo recombination with electrons leading to the formation of singlet and triplet excitons, which drive further the chemistry of isolated guest molecules. Apparently, the exciton transfer (7) does not lead to significant population of high triplet excited states. This may be the reason for the low yield of HOCO radicals in a xenon matrix. In addition, we should mention that this yield may be somewhat underestimated due to possibility of rather efficient decomposition of HOCO under irradiation in xenon, even at relatively low absorbed doses (see Fig. 3a).

In contrast to HOCO, the CO_2/CO ratio exhibits a regular matrix dependence increasing within the row Ne < Ar < Kr < Xe. At least, for Ar, Kr and Xe this trend is expected from the external heavy atom effect, if the CO_2 precursor states are populated due to intersystem crossing and it is in qualitative agreement with the previously reported data on photolysis.[11] Meanwhile, the relatively high yield of CO_2 in all the matrices suggests also the involvement of another channel in the formation of this species. As mentioned above, this may be direct population of the T_2 triplet excited states of formic acid due to recombination, which is basically independent of the matrix *Z* number and does not exist in photolysis. A particularly low CO_2 yield in a neon matrix may be also partially explained by lower yield of the recombination-induced excited states, as discussed above. Meanwhile, we may note that there are no quantitative data for the formic acid photochemistry in this matrix.

One more result that should be commented is the dose dependence for the formation of different products. Basically, non-linear dose dependencies imply the involvement of secondary processes and the efficiency of such processes obviously increases with increasing the degree of parent molecule conversion. In the case of radiolysis in matrices, this simply means that the products compete with parent molecules for matrix excitons and holes. As seen from Fig. 2b and 3d, the degradation of HCOOH, as well as the production of CO, CO_2 and HOCO in neon increase linearly with the absorbed dose. It is not surprising since the total absorbed dose and the maximum conversion degree of formic acid are relatively low in this matrix, even at long irradiation time, so the role of secondary processes is small. Meanwhile, in all other matrices we reach high degree of formic acid decomposition (up to 70–80%) and its degradation is slowing down at high doses (Fig. 2b). Considering the behaviour of products at high doses, we may notice that the HOCO radical is the most radiation-sensitive species. Its yield shows a trend to saturate with the increasing absorbed dose (or degree of HCOOH decomposition) in argon and passes through maximum in krypton and xenon matrices (Fig. 3). The most probable secondary reaction of this radical in the excited state is decarboxylation:[45]

$$HOCO \rightarrow H + CO_2 \quad (15)$$

As shown in the previous section, the relative yields of CO and CO_2 reveal significantly different dose dependence in different matrices. Probably, this result is more illustrative, if we consider the CO_2/CO ratio as a function of HCOOH conversion degree (Fig. 4). This function is nearly constant for neon, slightly increases for argon, slightly decreases for krypton, and drastically drops for xenon. We believe that such effects may be explained by an interplay of secondary reactions. Indeed, as known from previous study,[40] CO_2 undergoes a moderately efficient decomposition under radiolysis in all the noble gas matrices:

$$CO_2 \rightarrow CO + O \quad (16)$$

This process leads to simultaneous increase in the production rate of CO and decrease of the CO_2 yield at high doses, which should result in pronounced decrease of the CO_2/CO ratio. On the other hand, reaction (15) gives an additional amount of CO_2 from HOCO, which should result in the opposite effect on the CO_2/CO ratio. Obviously, reaction (16) predominates in xenon at high doses, because the CO_2 yield in this matrix is quite high, whereas the production of HOCO is small over the whole dose range. This is in agreement with the observed prominent decrease of the CO_2/CO ratio. Meanwhile, in the case of krypton, the efficiency of these two processes may become comparable because of lower yield of CO_2 and higher yield of HOCO in the primary processes. As a result, we observe much less pronounced effect of the absorbed dose (or conversion degree) on the CO_2/CO ratio. Decrease of this ratio is clearly visible only at a high conversion degree, when the concentration of HOCO radicals is low. Furthermore, in the case of argon, the contribution of reaction (15) may be even more important at moderate doses that could be the reason for the observed slight increase of the CO_2/CO ratio in this system.

Astrochemical implications

Finally, we would like to consider possible implications of the results described above to the astrochemical studies. As was mentioned under introduction, formic acid is among the most abundant complex molecules detected in the interstellar medium. An intriguing and important question is the fate of such species under the action of ionizing radiation (in particular, high-energy cosmic rays) in terms of their stability and degradation pathways. In this work, we present evidence for the radiation-induced decomposition of formic acid yielding the HOCO radical in the solid phase. We believe that this previously undetected pathway could play a significant role in the chemical reactions occurring in the interstellar and cometary ices. Indeed, one may note that the method applied in our study is relevant for simulations of the interstellar solid-state radiation-driven chemistry. Actually, we have examined the impact of X-rays on isolated HCOOH molecules frozen in a low-temperature ice. Even though the medium (solid noble gas) is very different from realistic astrochemical ices, basically, it provides good opportunity for modelling the solid-state chemical reactions. Thus, in principle, one can expect the formation of the HOCO radical in molecular clouds containing sufficient amount of formic acid. To the best of our knowledge,

direct astronomical observation of HOCO radicals in the interstellar medium is still lacking, although $HOCO^+$ ions have been detected in numerous interstellar sightlines.[74] On the other hand, possible involvement of the HOCO radical in the interstellar chemistry is considered in several theoretical studies and hypothetical reaction schemes, in particular with focus on the pathways of amino acid generation.[75,76] One may speculate that the route of chemical evolution from carboxylic acids to amino acids may include the radiation-induced fragmentation of the simplest carboxylic acids followed by the reaction of HOCO + R′ yielding R′–COOH, where R′ is an NH_2-containing radical or its precursor. This idea is somewhat supported by recent observations of Zins and Krim,[30] where the formation of the $NCCH_2COOH$ species was presumably detected as a result of UV photolysis of the $HCOOH\cdots CH_3CN$ intermolecular complex in a low-temperature neon matrix. Undoubtedly, direct astronomical evidence for neutral HOCO in an interstellar medium is required for further discussion on this issue.

Conclusions

In summary, we have first studied the radiation-induced decomposition of formic acid in various noble gas matrices, which revealed substantial difference between the radiolysis and UV photolysis of this molecule under matrix isolation conditions. The results obtained provide evidence for an additional primary decomposition channel (not known for photolysis), namely, the formation of HOCO radicals. The contribution of this channel is strongly dependent on the matrix used and, in the case of krypton, its yield is comparable to that of CO. In addition, we have demonstrated that the CO_2/CO production ratio under radiolysis is much higher than that reported for a 193 nm photolysis.[11] The matrix effect on this ratio is qualitatively consistent with the explanation proposed by Lundell and Räsänen[11] based on the heavy atom effect on the intersystem crossing. On the other hand, apparently, there are additional channels for the formation of the CO_2 precursor states under radiolysis, which do not occur in a 193 nm photolysis. The results obtained in our study can be explained by the involvement of high-energy recombination-induced excited states and direct population of triplet excited states, which are not produced under UV photolysis. In particular, it is suggested that the HOCO radical could result from high triplet excited states, either directly or through internal conversion to a vibrationally hot T_1 state. The finding of this reaction path is significant, particularly, for astrochemical consideration of the formic acid evolution in interstellar ices since it can make a bridge for better understanding of the reaction channels involved in the prebiotic evolution of matter. In this respect it provides a challenge for a radioastronomic search for possible manifestation of HOCO in the interstellar medium.

Acknowledgements

This work was supported by the Russian Science Foundation (project no. 14-13-01266). We are thankful to F. F. Sukhov and I. V. Tyulpina for contribution to the experimental technique.

References

1 H. C. Ramsperger and C. W. Porter, *J. Am. Chem. Soc.*, 1926, **48**, 1267–1273.
2 R. Gorden, Jr. and P. Ausloos, *J. Phys. Chem.*, 1961, **65**, 1033–1037.
3 D. L. Singleton, G. Paraskevopoulos and R. S. Irwin, *J. Phys. Chem.*, 1990, **94**, 695–699.
4 R. S. Irwin, D. L. Singleton, G. Paraskevopoulos and R. Mclaren, *Int. J. Chem. Kinet.*, 1994, **26**, 219–225.
5 M. Brouard, J. P. Simons and J.-X. Wang, *Faraday Discuss. Chem. Soc.*, 1991, **91**, 63–72.
6 H. Su, Y. He, F. Kong, W. Fang and R. Liu, *J. Chem. Phys.*, 2000, **113**, 1891–1897.
7 S. R. Langford, A. D. Batten, M. Kono and M. N. R. Ashfold, *J. Chem. Soc., Faraday Trans.*, 1997, **93**, 3757–3764.
8 C. H. Kwon, M. H. Choi, H. Hwang and H. L. Kim, *Bull. Korean Chem. Soc.*, 2012, **33**, 728–730.
9 M. Schwell, F. Dulieu, H.-W. Jochims, J.-H. Fillion, J.-L. Lemaire, H. Baumgärtel and S. Leach, *J. Phys. Chem. A*, 2002, **106**, 10908–10918.
10 J. Lundell and M. Räsänen, *J. Phys. Chem.*, 1995, **99**, 14301–14308.
11 J. Lundell and M. Räsänen, *J. Mol. Struct.*, 1997, **436/437**, 349–358.
12 L. Khriachtchev, E. Maçôas, M. Pettersson and M. Räsänen, *J. Am. Chem. Soc.*, 2002, **124**, 10994–10995.
13 A. Olbert-Majkut, J. Ahokas, J. Lundell and M. Pettersson, *Phys. Chem. Chem. Phys.*, 2010, **12**, 7138–7147.
14 K. A. Kufeld, W. R. Wonderly, L. O. Paulson, S. C. Kettwich and D. T. Anderson, *J. Phys. Chem. Lett.*, 2012, **3**, 342–347.
15 H.-Y. He and W.-H. Fang, *J. Am. Chem. Soc.*, 2003, **125**, 16139–16147.
16 Y. Kurosaki, K. Yokoyama and Y. Teranishi, *Chem. Phys.*, 2005, **308**, 325–334.
17 E. Martínez-Núñez, S. A. Vázquez, I. Borges, Jr., A. B. Rocha, C. M. Estévez, J. F. Castillo and F. J. Aoiz, *J. Phys. Chem. A*, 2005, **109**, 2836–2839.
18 I. Borges, Jr., A. B. Rocha, E. Martínez-Núñez and S. Vázquez, *Chem. Phys. Lett.*, 2005, **407**, 166–170.
19 E. Martínez-Núñez, S. Vázquez, G. Granucci, M. Persico and C. M. Estevez, *Chem. Phys. Lett.*, 2005, **412**, 35–40.
20 J. Novak, M. Mališ, A. Prlj, I. Ljubić, O. Kühn and N. Došlić, *J. Phys. Chem. A*, 2012, **116**, 11467–11475.
21 S. Maeda, T. Taketsugu and K. Morokuma, *J. Phys. Chem. Lett.*, 2012, **3**, 1900–1907.
22 J. Crovisier and D. Bockelée-Morvan, *Space Sci. Rev.*, 1999, **90**, 19–32.
23 P. E. Ehrenfreund and S. B. Charnley, *Annu. Rev. Astron. Astrophys.*, 2000, **38**, 427–483.
24 H. M. Boechat-Roberty, S. Pilling and A. C. F. Santos, *Astron. Astrophys.*, 2005, **438**, 915–922.
25 S. Pilling, A. C. F. Santos, W. Wolff, M. M. Sant'Anna, A. L. F. Barros, G. G. B. de Souza, N. V. de Castro Faria and H. M. Boechat-Roberty, *Mon. Not. R. Astron. Soc.*, 2006, **372**, 1379–1388.

26 D. P. P. Andrade, H. M. Boechat-Roberty, E. F. da Silveira, S. Pilling, P. Iza, R. Martinez, L. S. Farenzena, M. G. P. Homem and M. L. M. Rocco, *J. Phys. Chem. C*, 2008, **112**, 11954–11961.
27 R. Guillemin, W. C. Stolte and D. W. Lindle, *J. Phys. B: At., Mol. Opt. Phys.*, 2009, **42**, 12510.
28 D. P. P. Andrade, H. M. Boechat-Roberty, S. Pilling, E. F. da Silveira and M. L. M. Rocco, *Surf. Sci.*, 2009, **603**, 3301–3306.
29 D. P. P. Andrade, A. L. F. de Barros, S. Pilling, A. Domaracka, H. Rothard, P. Boduch and E. F. da Silveira, *Mon. Not. R. Astron. Soc.*, 2013, **430**, 787–796.
30 E. L. Zins and L. Krim, *Phys. Chem. Chem. Phys.*, 2014, **16**, 3388–3398.
31 V. I. Feldman, F. F. Sukhov, N. A. Slovokhotova and V. P. Bazov, *Radiat. Phys. Chem.*, 1996, **48**, 261–269.
32 V. I. Feldman, *Acta Chem. Scand.*, 1997, **51**, 181–192.
33 V. I. Feldman, *Radiat. Phys. Chem.*, 1999, **55**, 565–571.
34 V. I. Feldman, in *EPR of Free Radicals in Solids II. Trends in Applications and Methods*, ed. A. Lund and M. Shiotani, Springer, 2013, 2nd edn, pp. 25–69.
35 V. I. Feldman, F. F. Sukhov and A. Yu. Orlov, *Chem. Phys. Lett.*, 1999, **300**, 713–718.
36 V. Feldman, F. Sukhov, A. Orlov and I. Tyulpina, *Phys. Chem. Chem. Phys.*, 2003, **5**, 1769–1774.
37 V. I. Feldman, F. F. Sukhov, A. Yu. Orlov and N. A. Shmakova, *J. Phys. Chem. A*, 2000, **104**, 3792–3799.
38 V. I. Feldman, F. F. Sukhov, A. Yu. Orlov, I. V. Tyulpina and V. K. Ivanchenko, *Radiat. Phys. Chem.*, 2006, **75**, 106–114.
39 V. I. Feldman, F. F. Sukhov, E. A. Logacheva, A. Yu. Orlov, I. V. Tyulpina and D. A. Tyurin, *Chem. Phys. Lett.*, 2007, **437**, 207–211.
40 S. V. Ryazantsev and V. I. Feldman, *J. Phys. Chem. A*, 2015, **119**, 2578–2586.
41 V. I. Feldman, A. V. Kobzarenko, A. Y. Orlov and F. F. Sukhov, *Low Temp. Phys.*, 2012, **38**, 766–773.
42 S. V. Ryazantsev, A. V. Kobzarenko and V. I. Feldman, *J. Chem. Phys.*, 2013, **139**, 124315.
43 S. V. Kameneva, A. V. Kobzarenko and V. I. Feldman, *Radiat. Phys. Chem.*, 2015, **110**, 17–23.
44 V. I. Feldman, in *Applications of EPR in Radiation Research*, ed. A. Lund and M. Shiotani, Springer, 2014, pp. 151–188.
45 M. E. Jacox, *J. Chem. Phys.*, 1988, **88**, 4598–4607.
46 R. L. Redington, *J. Mol. Spectrosc.*, 1977, **65**, 171–189.
47 I. D. Reva, A. M. Plokhotnichenko, E. D. Radchenko, G. G. Sheina and Y. P. Blagoi, *Spectrochim. Acta, Part A*, 1994, **50**, 1107–1111.
48 M. Pettersson, J. Lundell, L. Khriachtchev and M. Räsänen, *J. Am. Chem. Soc.*, 1997, **119**, 11715–11716.
49 E. M. S. Maçôas, J. Lundell, M. Pettersson, L. Khriachtchev, R. Fausto and M. Räsänen, *J. Mol. Spectrosc.*, 2003, **219**, 70–80.
50 L. George and W. Sander, *Spectrochim. Acta, Part A*, 2004, **60**, 3225–3232.
51 K. Marushkevich, L. Khriachtchev, J. Lundell and M. Räsänen, *J. Am. Chem. Soc.*, 2006, **128**, 12060–12061.
52 K. Marushkevich, L. Khriachtchev and M. Räsänen, *J. Phys. Chem. A*, 2007, **111**, 2040–2042.
53 K. Marushkevich, L. Khriachtchev, J. Lundell, A. Domanskaya and M. Räsänen, *J. Phys. Chem. A*, 2010, **114**, 3495–3502.
54 K. Marushkevich, M. Siltanen, M. Räsänen, L. Halonen and L. Khriachtchev, *J. Phys. Chem. Lett.*, 2011, **2**, 695–699.
55 K. Marushkevich, L. Khriachtchev, M. Räsänen, M. Melavuori and J. Lundell, *J. Phys. Chem. A*, 2012, **116**, 2101–2108.
56 F. Ito, *J. Mol. Struct.*, 2015, **1091**, 203–209.
57 D. Forney, M. E. Jacox and W. E. Thompson, *J. Chem. Phys.*, 2003, **119**, 10814–10823.
58 H. M. Kunttu and J. A. Seetula, *Chem. Phys.*, 1994, **189**, 273–292.
59 J. H. Hubbel and S. M. Seltzer, *Tables of x-ray mass attenuation coefficients and mass energy-absorption coefficients from 1 keV to 20 MeV for elements Z = 1 to 92 and 48 additional substances of dosimetric interest*, http://www.nist.gov/pml/data/xraycoef.
60 X. Huang, R. C. Fortenberry, Y. Wang, J. S. Francisco, T. D. Crawford, J. M. Bowman and T. J. Lee, *J. Phys. Chem. A*, 2013, **117**, 6932–6939.
61 G. J. Jiang, W. B. Person and K. G. Brown, *J. Chem. Phys.*, 1975, **62**, 1201–1211.
62 Q. Cao, S. Berski, Z. Latajka, M. Räsänen and L. Khriachtchev, *Phys. Chem. Chem. Phys.*, 2014, **16**, 5993–6001.
63 Q. Cao, S. Berski, M. Räsänen, Z. Latajka and L. Khriachtchev, *J. Phys. Chem. A*, 2013, **117**, 4385–4393.
64 M. Pettersson, J. Lundell and M. Räsänen, *J. Chem. Phys.*, 1995, **103**, 205–210.
65 V. I. Feldman and F. F. Sukhov, *Chem. Phys. Lett.*, 1996, **255**, 425–430.
66 M. Zhang and L. Sheng, *Phys. Chem. Chem. Phys.*, 2014, **16**, 196–203.
67 J. S. Francisco, J. T. Muckerman and H.-G. Yu, *Acc. Chem. Res.*, 2010, **43**, 1519–1526.
68 NIST Standard Reference Database 69: *NIST Chemistry WebBook*, http://webbook.nist.gov/chemistry/.
69 Y. Valadbeigi and H. Farrokhpour, *Int. J. Quantum Chem.*, 2013, **113**, 1717–1721.
70 E. V. Saenko, D. N. Laikov, I. A. Baranova and V. I. Feldman, *J. Chem. Phys.*, 2011, **135**, 101103.
71 L. Sanche, *Nucl. Instrum. Methods Phys. Res., Sect. B*, 2003, **208**, 4–10.
72 L. B. Knight, Jr., *Acc. Chem. Res.*, 1986, **19**, 313–321.
73 V. I. Feldman, F. F. Sukhov, A. Yu. Orlov, I. V. Tyul'pina, E. A. Logacheva and D. A. Tyurin, *Russ. Chem. Bull.*, 2005, **54**, 1458–1466.
74 N. Sakai, T. Sakai, Y. Aikawa and S. Yamamoto, *Astrophys. J.*, 2008, **675**, L89–L92 and references therein.
75 D. E. Woon, *Astrophys. J.*, 2002, **571**, L177–L180.
76 P. D. Holtom, C. J. Bennett, Y. Osamura, N. J. Mason and R. I. Kaiser, *Astrophys. J.*, 2005, **626**, 940–952.

